BRAIN
ORIGINAL ARTICLE

Common molecular mechanisms of *SLC6A1* variant-mediated neurodevelopmental disorders in astrocytes and neurons

Felicia Mermer,[1,†] Sarah Poliquin,[2,3,†] Kathryn Rigsby,[3] Anuj Rastogi,[4] Wangzhen Shen,[1] Alejandra Romero-Morales,[4,5] Gerald Nwosu,[1,6] Patrick McGrath,[7] Scott Demerast,[7] Jason Aoto,[8] Ganna Bilousova,[9] Dennis Lal,[10] Vivian Gama[2,3,4,5] and Jing-Qiong Kang[1,2,3,11,12]

†These authors contributed equally to this work.

See Cheng and Carvill (doi:10.1093/brain/awab259) for a scientific commentary on this article.

Solute carrier family 6 member 1 (*SLC6A1*) is abundantly expressed in the developing brain even before the CNS is formed. Its encoded GABA transporter 1 (GAT-1) is responsible for the reuptake of GABA into presynaptic neurons and glia, thereby modulating neurotransmission. GAT-1 is expressed globally in the brain, in both astrocytes and neurons. The GABA uptake function of GAT-1 in neurons cannot be compensated for by other GABA transporters, while the function in glia can be partially replaced by GABA transporter 3. Recently, many variants in *SLC6A1* have been associated with a spectrum of epilepsy syndromes and neurodevelopmental disorders, including myoclonic atonic epilepsy, childhood absence epilepsy, autism, and intellectual disability, but the pathomechanisms associated with these phenotypes remain unclear. The presence of GAT-1 in both neurons and astrocytes further obscures the role of abnormal GAT-1 in the heterogeneous disease phenotype manifestations.

Here we examine the impact on transporter trafficking and function of 22 *SLC6A1* variants identified in patients with a broad spectrum of phenotypes. We also evaluate changes in protein expression and subcellular localization of the variant GAT-1 in various cell types, including neurons and astrocytes derived from human patient induced pluripotent stem cells.

We found that a partial or complete loss-of-function represents a common disease mechanism, although the extent of GABA uptake reduction is variable. The reduced GABA uptake appears to be due to reduced cell surface expression of the variant transporter caused by variant protein misfolding, endoplasmic reticulum retention, and subsequent degradation. Although the extent of reduction of the total protein, surface protein, and the GABA uptake level of the variant transporters is variable, the loss of GABA uptake function and endoplasmic reticulum retention is consistent across induced pluripotent stem cell-derived cell types, including astrocytes and neurons, for the surveyed variants. Interestingly, we did not find a clear correlation of GABA uptake function and the disease phenotypes, such as myoclonic atonic epilepsy versus developmental delay, in this study. Together, our study suggests that impaired transporter protein trafficking and surface expression are the major disease-associated mechanisms associated with pathogenic *SLC6A1* variants.

Our results resemble findings from pathogenic variants in other genes affecting the GABA pathway, such as GABA$_A$ receptors. This study provides critical insight into therapeutic developments for *SLC6A1* variant-mediated disorders and implicates that boosting transporter function by either genetic or pharmacological approaches would be beneficial.

1 Department of Neurology, Vanderbilt University Medical Center, Nashville, TN 37232, USA
2 Neuroscience Graduate Program, Vanderbilt University, Nashville, TN 37232, USA
3 Vanderbilt Brain Institute, Nashville, TN 37232, USA
4 Department of Cell and Developmental Biology, Vanderbilt University Medical Center, Nashville, TN 37232, USA
5 Vanderbilt Center for Stem Cell Biology, Nashville, TN 37232, USA
6 Vanderbilt-Meharry Alliance Vanderbilt University, Nashville, TN 37232, USA
7 Department of Pediatrics, University of Colorado Anschutz Medical Campus, Aurora, CO 80045, USA
8 Department of Pharmacology, University of Colorado Anschutz Medical Campus, Aurora, CO 80045, USA
9 Department of Dermatology, Charles C. Gates Center for Regenerative Medicine, University of Colorado Anschutz Medical Campus, Aurora, CO 80045, USA
10 Cleveland Clinic Genomic Medicine Institute and Neurological Institute, Cleveland, OH 44195, USA
11 Department of Pharmacology, Vanderbilt University, Nashville, TN 37232, USA
12 Vanderbilt Kennedy Center of Human Development, Nashville, TN 37232, USA

Correspondence to: Jing-Qiong Kang
Department of Neurology and Pharmacology
Vanderbilt University Medical Center, 465 21st Ave South
Nashville, TN 37232, USA
E-mail: jingqiong.kang@vumc.org; jingqiong.kang@vanderbilt.edu

Introduction

Gamma-aminobutyric acid (GABA), the major inhibitory neurotransmitter, and its transporters and receptors work in concert to regulate GABA signalling, neurotransmission, plasticity, and cortical information processing, which are essential for normal brain development and homeostasis. GABA is a neurotrophic signal that regulates neural stem cell proliferation,[1,2] and GABA activation of GABA$_A$ receptors is essential for synaptogenesis.[3] The GABA transporter-1 (GAT-1), encoded by *SLC6A1*, is one of the major GABA transporters in the brain, and a member of a large family of 12-transmembane domain Na$^+$/Cl$^-$-coupled transporters including GAT-2, GAT-3 and betain/GAT 1 (BGT1). GAT-1 co-transports sodium, chloride, and GABA at a ratio of 2 Na:1 Cl:1 GABA.[4,5] It has been demonstrated that impaired GABAergic signalling is a converging pathway of pathophysiology in genetic epilepsy and autism as well as in other neurodevelopmental disorders.[6] Likewise, GABAergic signalling is an established therapeutic target for those disorders.[7]

GAT-1 is expressed by both inhibitory neurons and astrocytes, while *SLC6A1* (GAT-1) mRNA has been reportedly expressed throughout the brain cortex.[8] Among the total four types of GABA transporters, GAT-1–3 and BGT1, GAT-1 is the predominant form in the forebrain.[9,10] In the rat developing brain, *Slc5a1* (GAT-1) mRNA was detected from embryonic brain Day 13,[11] consistent with its critical role in brain development. Immunohistochemical studies showed that GAT-1 is not only expressed in GABAergic neurons, but also in non-GABAergic cells and glia, though the exact role of how the GAT-1 modulates neurotransmission and contributes to the overall GABA homeostasis is unclear. It has been established that the GABA uptake function in neurons is largely mediated by GAT-1 and could not be compensated for by other GATs. In addition, there was no redistribution of GAT-3 in the absence of GAT-1. In GAT-1 knockout mice, GABA uptake is diminished with altered tonic and phasic GABAergic neurotransmission, but there is little or no compensatory change in other proteins or structures related to GABA neurotransmission.[12,13]

Recently, variants in *SLC6A1* have been reported to be associated with a spectrum of epilepsy syndromes, autism, and impaired cognition.[14–20] It is of note that the clinical phenotypes associated with *SLC6A1* variants are similar to those with GABA$_A$ receptor gene variants, especially *GABRB3*. It is unknown how the variants alter GABA uptake function of the variant GAT-1 nor how this alteration subsequently modulates the function of the GABA$_A$ receptor chronically in the brain. It has been demonstrated that GAT-1 blockade or genetic deletion specifically impairs long-term potentiation (LTP) induced by theta burst stimulation,[21] implicating the role of GAT-1 in cognition. It is intriguing that the pharmacological compound tiagabine, a GAT-1 inhibitor, has been used for treating focal epilepsy.[22] This paradox complicates the picture of the pathophysiology and therapeutic intervention for *SLC6A1*-mediated seizure phenotypes.

In this study, we report the impact of 22 variants in *SLC6A1* associated with a wide spectrum of neurodevelopmental disorders, from myoclonic atonic epilepsy, childhood absence epilepsy, autism, and intellectual disability. Because of glial and neuronal expression of GAT-1, we characterized the function and expression of *SLC6A1* variants in both neurons and astrocytes. We evaluated the impact of a representative variant in patient-derived induced pluripotent stem cells (iPSCs), neural progenitor cells (NPCs), astrocytes, and post-mitotic GABAergic inhibitory neurons. This study identifies common pathophysiological mechanisms for *SLC6A1* variants across cell types in both mouse and human iPSC-derived cells using multidisciplinary approaches. Our report provides critical insight into how *SLC6A1* variants affect GAT-1 functioning and trafficking and how to design mechanism-based treatment options.

Materials and methods

Patient information

The patient variants are combined from various sources, including the patient foundation SLC6A1 Connect, the Human Mutation

Gene Database website, and previously published studies. For variants that are not publicly available, patient consent was obtained according to the institutional review board.

Cloning of GABA transporter 1

The plasmid cDNA encoding enhanced yellow fluorescent protein (YFP)-tagged rat GAT-1 has been previously described.[23–25] The coding region of rGAT-1 was inserted into pEYFP-C1 (Clontech). The QuikChange Site-directed Mutagenesis kit was used to introduce the GAT-1 variants into a wild-type GAT-1 plasmid. The product was then amplified via PCR, transformed using DH5α competent cells, and plated. A clone was chosen and grown overnight. All the GAT-1 variants were confirmed by DNA sequencing. Both the wild-type and the variant cDNAs were prepared with a Qiagen Maxiprep kit.

Neuronal and astrocyte cultures and transfections

Mouse cortical neuronal cultures and transfection were prepared as previously described.[26,27] For mouse cortical astrocytes, the cortices of postnatal Day 0–3 pups were dissected. The tissues were minced after removing the meninges and then digested with 0.25% trypsin for 10 min at 37°C. The cells were then maintained in Dulbecco's modified Eagle medium (DMEM) supplemented with 10% foetal bovine serum (FBS) and 1% penicillin/streptomycin. The details for astrocytes culture and transfection are described in the Supplementary material.

Human patient-derived iPSCs, NPCs, astrocytes and neurons

The patient-derived and CRISPR-corrected iPSCs were obtained in collaboration with Dr Jason Aoto's lab (University of Colorado). The normal human iPSC clone was purchased from Thermo Fisher (A18945). The detailed iPSC culture, solutions, and differentiation protocols are described in the Supplementary material. Briefly, the corrected and patient cell lines were maintained in plates coated with Geltrex® (1:50 DMEM/F12) overnight using mTeSR (StemCell Technologies). The media was refreshed daily for iPSCs. The differentiation of NPCs was induced by STEMdiff™ SMADi Neural Induction kit from StemCell Technologies. The differentiation of astrocytes was initiated using the Astrocyte medium (ScienCell) for 27–30 days,[28] and the cells were passaged at ∼70% confluence. The cortical inhibitory neurons were prepared following previous reports.[29] The neurons were harvested for experiments at Day 60–65 after differentiation. Neuronal identity was validated by immunostaining with NeuN, DLX, synapsin and synaptophysin. Neuronal differentiations were initiated from the NPCs at Day 10 from passage 2 after neuronal induction. The differentiation of astrocytes was initiated at NPC Day 5 from passage 1. The experiments were carried out between 27 to 30 days after differentiation for astrocytes or 60 to 65 days after differentiation for neurons.

Radioactive ^{3}H-labelled GABA uptake assay

The radioactive ^{3}H-labelled GABA uptake assay in HEK293T cells, mouse neurons and astrocytes, human patient-derived iPSCs, NPCs, astrocytes and neurons was modified from the protocol used in our previous studies,[30] which is detailed in the Supplementary material. The protocols for GABA reuptake assay in cultured mouse astrocytes, neurons, or iPSC-derived cells were modified from the GABA uptake protocol on HEK293T cells. Control dishes treated with the GAT-1 inhibitors Cl-966 and NNC-711 were included for each experiment.

Confocal microscopy and image acquisition

Live cell confocal microscopy was performed using an inverted Zeiss laser scanning microscope (Model 510) with a 63× 1.4 NA oil immersion lens, 2–2.5× zoom, and multi-track excitation.[31] Cells were plated on poly-L-ornithine and laminin-coated coverslips or glass-bottom imaging dishes at the density of $1–2 \times 10^5$ cells per dish and co-transfected with 1 μg of the wild-type or the variant GAT-1 plasmids per 35-mm glass-bottomed culture dish with PEI, as per our standard laboratory protocol. For immunohistochemistry on iPSCs, astrocytes and iPSC-derived neurons, rabbit IgG was recognized by Cy3 (red) while mouse IgG was visualized by Alexa-488 (green). The cell nuclei were stained with the cell nuclei marker TO-PRO-3. All images were obtained from single confocal sections averaged from eight times to reduce noise, except when otherwise specified.

Measurement of surface and total expression of GAT-1 using flow cytometry

The protocol used for measurement of surface and total expression of GAT-1 using flow cytometry has been described previously for studies on GABA$_A$ receptor variants.[27]

Ethics statement

All animals and related experiments in this study were approved by the Vanderbilt University IACUC.

Statistical analysis

Data are expressed as mean ± standard error of the mean (SEM). Proteins were quantified by Odyssey software and data were normalized to loading controls and then to wild-type subunit proteins, which was arbitrarily taken as 1 in each experiment. Fluorescence intensities from confocal microscopy experiments were determined using MetaMorph® imaging software, and the measurements were carried out in ImageJ as modified from previous reports.[26,31–33] For statistical significance, we used one-way ANOVA with Newman-Keuls test or Student's unpaired t-test. In some cases, one sample t-test or unpaired t-test was performed (GraphPad Prism, La Jolla, CA), and statistical significance was taken as $P < 0.05$.

Data availability

The data supporting the findings of this study are available within the article and its Supplementary material.

Results

SLC6A1 variants are associated with a wide spectrum of neurodevelopmental disorders

Numerous variants in *SLC6A1* have been identified to date, and these variants are associated with various epilepsy syndromes, including myoclonic atonic epilepsy, childhood absence epilepsy, autism, intellectual disability, and developmental delay (https://ncbi.nlm.nih.gov/clinvar/) (Fig. 1A). We selected variants from previously reported studies,[34–36] ClinVar, Human Mutation Gene Database websites, and SLC6A1 Connect, which consist of missense, nonsense and frameshift variants located in various domains of the protein, and conducted functional assays. The variants are associated with the predominant phenotypes myoclonic atonic epilepsy, intellectual disability, or autism, or less frequently with phenotypes such as Lennox-Gastaut syndrome and
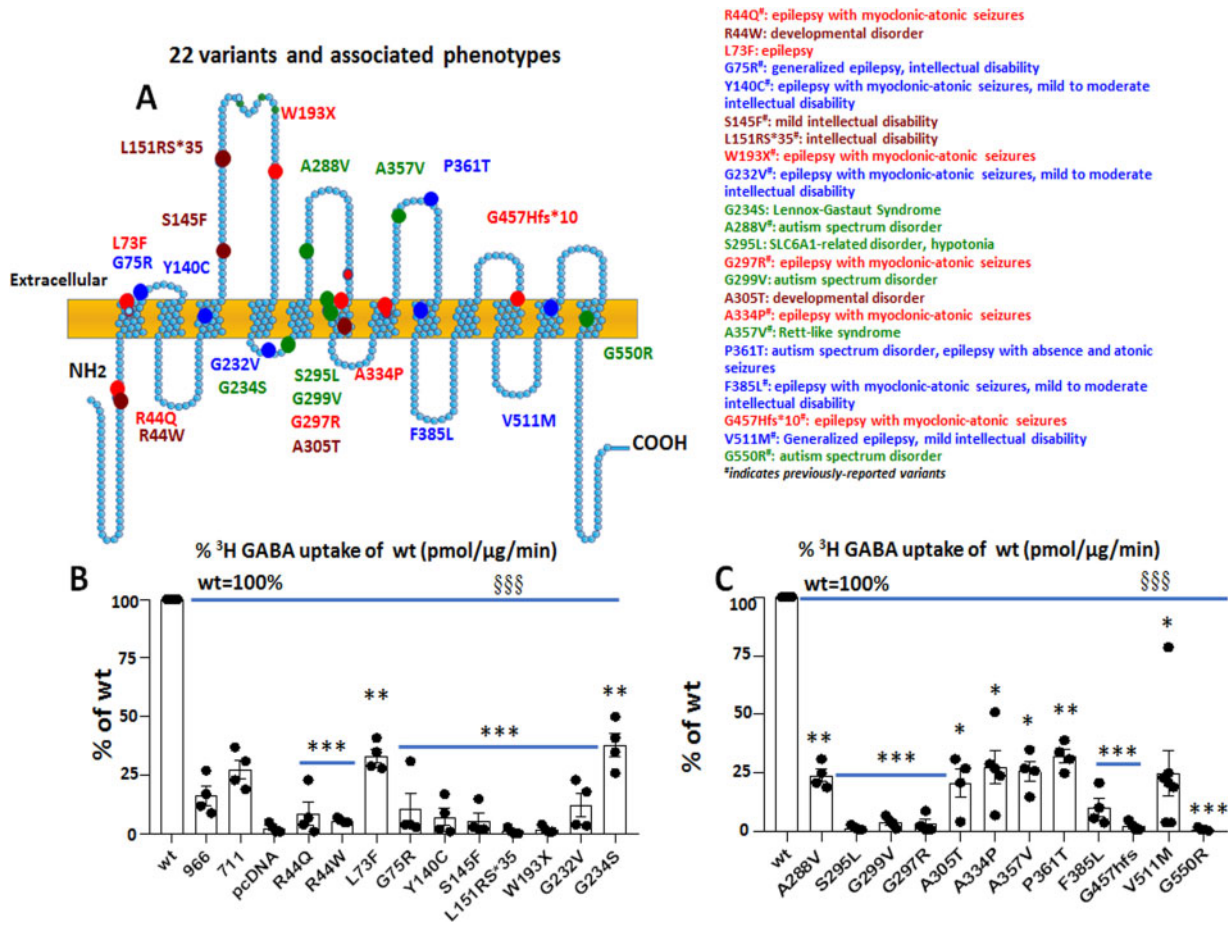
Figure 1 Partial or complete loss of GABA reuptake activity is a common phenomenon across GABA transporter 1 (encoded by *SLC6A1*) variations associated with a wide spectrum of epilepsy syndromes and neurodevelopmental disorders. (A) Schematic presentation of variant GABA transporter 1 (GAT-1) protein topology and locations of variations in human *SLC6A1* associated with various epilepsy syndromes and neurodevelopmental disorders. These variations are distributed in various locations and domains of the encoded GAT-1 protein peptide. The coloured dots represent the relative locations of the disease-related variations. #Previously reported variants. **(B** and **C)** HEK293T cells were transfected with the empty vector pcDNA, wild-type, or the variant GAT-1^{YFP} for 48 h. The graphs represent the altered GABA reuptake function of the variant GAT-1 encoded by 22 different *SLC6A1* variations in HEK293T cells measured by the high-throughput ^{3}H radiolabelling GABA uptake on a liquid scintillator with QuantaSmart. '966' indicates the wild-type treated with GAT-1 inhibitor Cl-966 (50 μM), and 'NNC-711' indicates the wild-type treated with NNC-711 (70 μM) for 30 min before preincubation. $n = 4$ different transfections, $^{§§§}P < 0.001$ overall variations versus wild-type, $^*P < 0.05$, $^{**}P < 0.01$, $^{***}P < 0.001$ versus wild-type, one-way ANOVA and Newman-Keuls test. Values are expressed as mean ± SEM.

generalized epilepsy with febrile seizures plus. All these variants are likely pathogenic. We included variants that were previously reported[24,25, 34–36] or registered in SLC6A1 Connect in individuals with a wide spectrum of neurodevelopmental disorders, though we did not have sufficient information to characterize them per the ACMG criteria.[37] We transfected the wild-type or the variant GAT-1^{YFP} cDNAs in HEK293T cells and evaluated the GABA uptake activity. The GAT-1 inhibitors Cl-966 (50 μM) and NNC-711 (70 μM) were applied to the cells expressing the wild-type GAT-1^{YFP} cDNAs for 30 min before preincubation and washed off before testing. The radioactivity in conditions treated with the GAT-1 inhibitors was reduced, thus serving as a negative control.

All surveyed variants in *SLC6A1* resulted in a partial or complete loss of GABA uptake function

Variants in *SLC6A1*, regardless of the associated clinical phenotypes, had reduced GABA uptake function as measured by ^{3}H radiolabelling GABA uptake assay (Fig. 1B and C). The GABA uptake

activity from the untransfected HEK293T cells was taken as background and subtracted from the total scintillation counts in each condition. The reduction of GABA uptake in each variant has no clear correlation with the location of the variants in the protein peptide or disease phenotype. The variants reduced the GABA uptake activity to a level similar to that in the cells treated with GAT-1 inhibitor Cl-966 (∼20% of the wild-type GAT-1 activity) and NNC-711 (∼30% of the wild-type GAT-1 activity). We compared the variants in the extracellular or intracellular α-helix or transmembrane domain and found no clear correlation between the GABA uptake reduction and the variant location. We also compared the level of GABA uptake reduction in variants associated with different clinical phenotypes, but there was no clear correlation. The overall remaining level of the variant transporter function ranges from almost none to ∼40% of the wild-type for all surveyed variants (Fig. 1B and C). The complete loss-of-function variants include missense, nonsense, and frameshift variants. Some other variants had reduced, but not complete loss of GABA uptake function, suggesting that *SLC6A1* pathogenic variants could cause partial or complete loss-of-function of GAT-1.
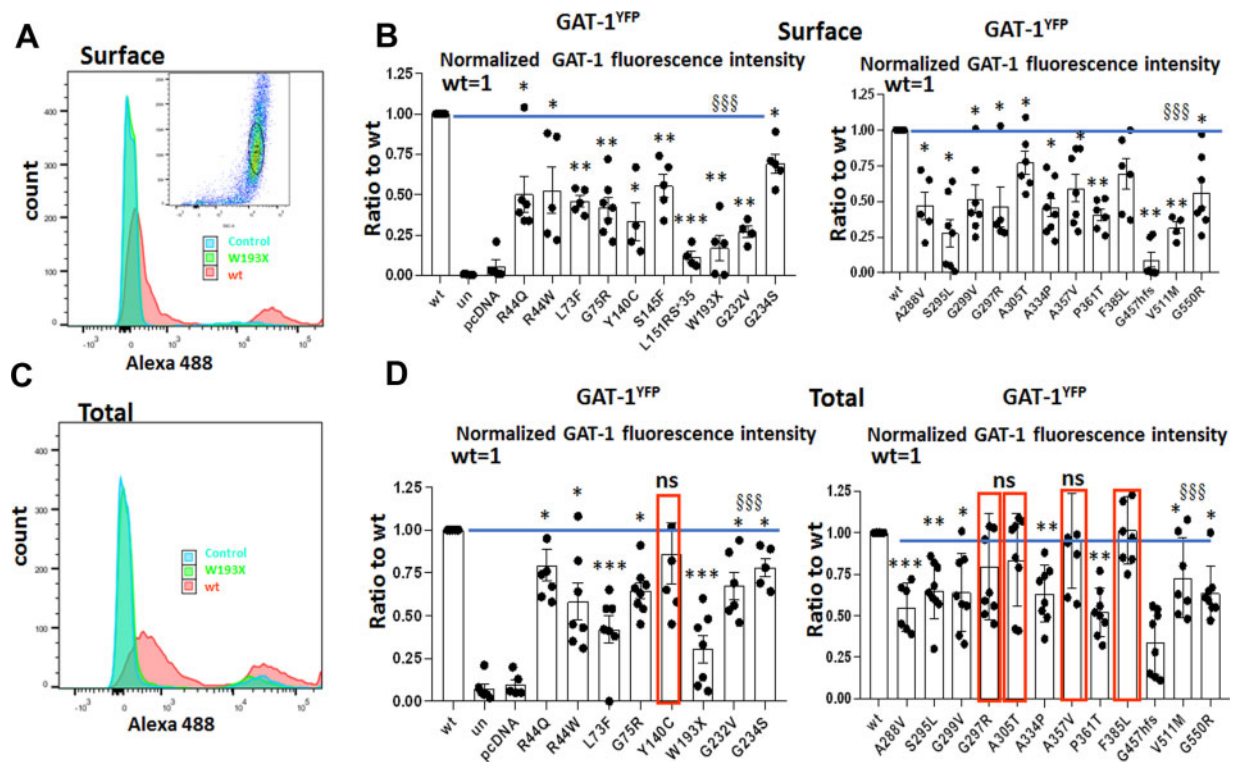
Figure 2 Altered surface and total expression of variant GAT-1 measured with a high-throughput flow cytometry. (**A** and **C**) The flow cytometry histograms depict surface (**A**) or total (**C**) expression of the wild-type and the variant GAT-1. HEK293T cells were transfected with the wild-type or the variant GAT-1^{YFP} using 3 μg of cDNAs with polyethylenimine (PEI) at a ratio of 1 μg cDNA to 2.5 μl PEI, with 3 μg cDNAs total. (**B** and **D**) The graphs showing the normalized cell surface (**B**) or total (**D**) expression of GAT-1^{YFP} from the cells expressing the wild-type or the variant transporters. The relative subunit expression level of GAT-1 in each variant transporter, as well as untransfected (only with PEI) and mock transfected (pcDNA), was normalized to that obtained from cells with transfection of the wild-type. In **D**, red boxed variants were not different from the wild-type. n = 4–7 different transfections, $^{§§§}P < 0.001$ overall variations versus wild-type, $^{*}P < 0.05$, $^{**}P < 0.01$, $^{***}P < 0.001$ versus wild-type, one-way ANOVA and Newman-Keuls test. Values are expressed as mean ± SEM.

SLC6A1 variants reduced surface expression with or without reducing total protein expression of the variant GAT-1

Reduced GABA uptake function could be due to reduced transporter protein trafficking to the cell surface, as observed in GABA$_A$ receptors[38,39] and other SLC6 family members. Trafficking deficiency can cause loss of or reduced protein presence on the cell surface, with or without reduction of the total protein. We thus determined the trafficking pattern of the YFP-tagged GAT-1 for multiple variants associated with different epilepsies and autism by expressing the wild-type or the variant GAT-1 cDNAs in HEK293T cells followed by a high throughput assay flow cytometry. As shown by the inset in Fig. 2A, a population of 10 000 non-aggregated cells was evaluated for each sample for fluorescence intensity. YFP-tagged GAT-1 was confirmed to have similar expression and function as the native GAT-1. The transfection efficiency was comparable across samples based on validation with biochemical approaches. The surface or total GAT-1 was evaluated in the cells from the same dish with or without membrane permeabilization per our standard laboratory protocol. We found that the surface expression level of GAT-1 was variable (Fig. 2A and B) but was consistently reduced for all surveyed variants (Fig. 2A and B), with the reductions ranging from ~100% to ~20% of wild-type (Fig. 2A and B). However, since the reduced cell surface expression may not represent the expression level of the variant GAT-1 at total level, we then evaluated the total expression of GAT-1 for the

variants. Similar to the surface level expression, the total GAT-1 expression was reduced for most variants (Fig. 2C and D). Five (Y140C, G297R, A305T, A357V and F385L) of the 22 variants had unaltered total protein expression. Similar to the surface expression, the reduction of GAT-1 total expression was variable among variants ranging from ~30% to ~85% of the wild-type. The GABA uptake, variant protein surface and total expression as well as the correlation of GABA uptake and protein expression for all surveyed variants are detailed in Supplementary Table 1.

SLC6A1 variants resulted in intracellular retention of variant GAT-1 and reduced GABA uptake function

GAT-1 is expressed in both neurons and astrocytes. We have previously identified the intracellular retention of epilepsy variants in GABA$_A$ receptor subunits in neurons,[40] but the expression pattern of a trafficking-deficient variant protein in astrocytes is unknown. We thus chose two representative variants to determine if the expression of the variant GAT-1 in cultured mouse neurons and astrocytes has a similar pattern. We chose these two variants because we have extensively studied them[25] and they are representative of partial or complete loss-of-function variants based on function and trafficking patterns. We expressed GAT-1^{YFP} or the variant GAT-1^{YFP} (S295L and P361T) in cultured mouse neurons or astrocytes. In live astrocytes, the variant GAT-1 had a distinct expression pattern compared with the wild-type. As evident in Fig. 3A, wild-type GAT-1^{YFP} had a smooth distribution of the
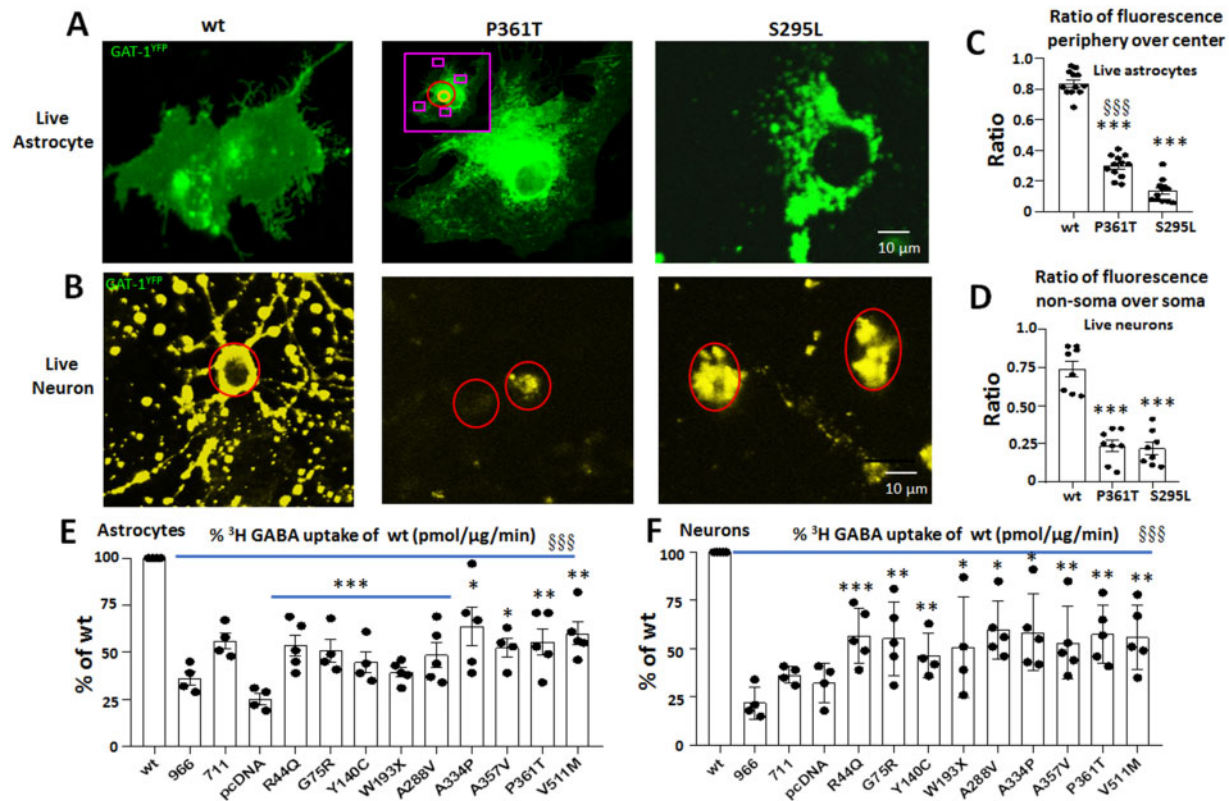
Figure 3 Reduced function of variant GAT-1 in live mouse cortical astrocytes and neurons. Mouse cortical neurons were cultured from postnatal Day 0 pups, while cortical astrocytes were cultured from postnatal Day 0–3 pups. (**A**) Astrocytes (passage 2) were transfected with the wild-type GAT-1^{YFP}, GAT-1(P361T)^{YFP} or GAT-1(S295L)^{YFP} with PEI and harvested at 48 h after transfection. (**B**) Neurons were transfected for the same conditions at Day 5–7 in culture with a calcium precipitation method and harvested for experiments at Day 15 in dish. The images show two representative variants (P361T) and (S295L) in live astrocytes (**A**) or in live neurons (**B**). (**C** and **D**) The GAT-1^{YFP} fluorescence in different subcellular compartments was quantified by MetaMorph®. (**C**) The GAT-1^{YFP} fluorescence in astrocytes was measured at the peripheral and central regions, as illustrated in the *inset* in the *middle* panel of **A**. The purple rectangle represents the peripheral region, the red circle represents the middle region, and the orange circle represents nuclei region, which was taken as background signal (*n* = 12 cells from four batches of cells). (**D**) The ratio of GAT-1^{YFP} fluorescence in dendrites versus soma was measured by sampling the region of somatic versus non-somatic region (*n* = 8 fields from three batches of cells). (**E** and **F**) Neurons or astrocytes were prepared in 35 mm dishes, and the GABA uptake function was evaluated with ^{3}H radiolabelling. The graph represents the relative activity of GABA uptake in mouse cortical astrocytes (**E**) or cortical neurons (**F**). In **C**–**F**, ***$P < 0.001$ versus wild-type, in **C**, §§§$P < 0.001$ versus S295L. In **E** and **F**, *n* = 4–5 transfections, §§§$P < 0.001$ overall variants versus wild-type, *$P < 0.05$, **$P < 0.01$. One-way ANOVA and Newman-Keuls test was used to determine significance compared to the wild-type condition and between variations. Values are expressed as mean ± SEM.

fluorescence throughout the astrocytes with minimally increased presence of the fluorescence around the cell nuclei in some cases. However, the variant GAT-1(P361T), a variant associated with epilepsy and autism, had increased presence of YFP fluorescence around the cell nuclei but only a faint fluorescence at the edge of the cells. For the variant GAT-1(S295L), the GAT-1 fluorescence was only present around the cell nuclei and was not visible at the edge of the cells (Fig. 3A). In live cortical neurons, the neurons expressing the wild-type GAT-1^{YFP} had a diffuse distribution of the fluorescence presented as puncta throughout the surveyed fields, while the GAT-1(P361T)^{YFP} had a reduced fluorescence signal with very few puncta. The GAT-1(S295L)^{YFP} had a strong YFP fluorescence localized in the neuronal somatic region in live neurons (Fig. 3B) but had very few puncta, similar to GAT-1(P361T)^{YFP}. In live astrocytes, the ratio of the YFP fluorescence at the periphery to the fluorescence in the central region around the nuclei was lower in both variants compared with the wild-type GAT-1 (0.84±0.023 for wild-type versus 0.30±0.024 for P361T versus 0.135±0.021 for S295L, *n* = 12 cells) (Fig. 3C). Consistent observation was made in live neurons expressing the wild-type and the variant GAT^{YFP} transporters. This pattern of reduced ratio of the YFP fluorescence

in the non-somatic region (neurites) versus soma was also observed in live neurons (Fig. 3D) (0.5086±0.06 for wild-type versus 0.22±0.031 for P361T and 0.196±0.025 for S295L, *n* = 8 cells). The cell body was confirmed by DIC imaging from transmitted light microscopy (Supplementary Fig. 1).

We then determined the GABA uptake function of the variant GAT-1 in both neurons and astrocytes cultured from mouse cortex (Fig. 3E and F). The neurons were transfected with the wild-type or the variant cDNAs 7 days before evaluation, while astrocytes were transfected 2 days before evaluation. We chose 10 variants across different domains of the GAT-1 protein peptide associated with different clinical phenotypes. The variant GAT-1 had reduced GABA uptake activity in both neurons and astrocytes, which is consistent with our observations in HEK293T cells. However, the magnitude of GABA uptake reduction is different among different cell types. The reduction of GABA reuptake function for variants ranges from ∼40% to ∼75% in astrocytes (Fig. 3E) and ∼40% to ∼60% in neurons (Fig. 3F). The differential magnitude of reduction between HEK293T and neural cells could be attributed to the endogenous variation in expression of GAT-1in different cell types and to transfection efficiency.
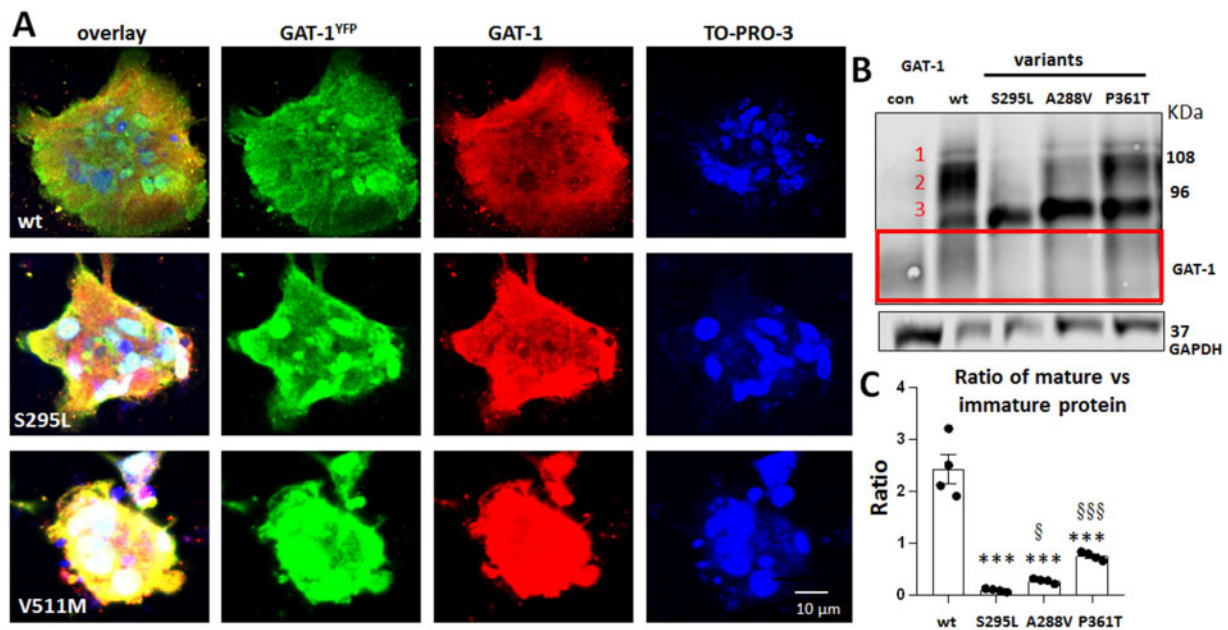
Figure 4 Variant GAT-1 is accumulated inside astrocytes and is immature due to glycosylation arrest. (**A**) Representative images of mouse cortical astrocytes expressing the wild-type or the variant GAT-1^{YFP} (S295L and V511M) for 48 h. The astrocytes were immunostained with a mouse monoclonal anti-GFP antibody, which recognizes GAT-1^{YFP}, and rabbit polyclonal GAT-1 antibody, which recognizes the transfected and endogenous GAT-1. Cell nuclei were stained with TO-PRO-3 (four batches of cultures with transfections). (**B**) The total lysates of astrocytes expressing the wild-type or variant GAT-1 were analysed by SDS-PAGE. The membrane was immunoblotted with a rabbit anti-GAT-1, which detects both the transfected and endogenous GAT-1 expressed in astrocytes. The red-boxed region represents the endogenous GAT-1 in astrocytes. (**C**) The graph represents the ratio of normalized integrated protein density values (IDVs) of the bands with higher molecular mass (Bands 1 and 2) over the lower band (Band 3). ***$P <$ 0.001 versus wild-type; $^{§}P <$ 0.05 and $^{§§§}P <$ 0.001 versus S295L. One-way ANOVA and Newman-Keuls test was used to determine the significance compared to the wild-type condition and between variants. Values are expressed as mean ± SEM.

SLC6A1 variants resulted in glycosylation arrest leading to decreased mature GAT-1 protein in astrocytes

Trafficking-deficient variants could result in protein glycosylation arrest, consequently resulting in less mature and endoplasmic reticulum (ER)-retained mutant protein.[26] We thus determined the expression of the variant GAT-1 at different glycosylation states. Since all the patients were heterozygous, we investigated if the variant transporters could interfere with the wild-type transporters. We transfected the wild-type or the variant GAT-1^{YFP} in astrocytes and probed the astrocytes for YFP and GAT-1 by immunofluorescence. GFP staining recognized the transfected wild-type or variant GAT-1 and GAT-1 staining recognized the total GAT-1 protein, including both the endogenously expressed and the transfected protein. The cell nuclei were stained with TO-PRO-3. Variant GAT-1 appeared aggregated in contrast to the wild-type that shows a smooth distribution throughout the cell body (Fig. 4A). Interestingly, the endogenous GAT-1 in the cells expressing the variant GAT-1 also appeared to be accumulated with the variant protein. This may suggest that the variant GAT-1 could oligomerize with the wild-type copy and somehow interfere with the wild-type transporter trafficking. We then studied the total protein expression in astrocytes (Fig. 4B and Supplementary Fig. 2). The wild-type GAT-1^{YFP} ran at two main bands: a main band at ~108 kDa and a lower band at 96 kDa, in contrast to three distinct bands observed in HEK293T cells. There was a faint band above the main band labelled as Band 1. GAT-1 protein has three glycosylation sites, with the predicted protein size—including the YFP tag—being 108, 96 and 90 kDa.[24] We then quantified the ratio of Bands 1 and 2 over Band 3 (Fig. 4C); all the variants had reduced ratio of the first and second bands over the third band (2.43±0.29 for wild-type; 0.088±0.015 for S295L;

0.27±0.021 for A288V; 0.75±0.04 for P361T). Interestingly, the ratios among the variants were different: the GAT-1(A288V) and GAT-1(P361T) variant proteins had a higher ratio than the variant GAT-1(S295L) protein. This suggests that different variants could have a different amount of mature protein on the cell surface, which consequently results in differing extents of reduction in GABA uptake function (Supplementary Table 1).

SLC6A1 variants cause reduced GABA reuptake activity in patient iPSC-derived cells

Comparative analysis of the results obtained in the mouse neural cells with human neurons and astrocytes is essential to address potential species differences in protein expression and function. We thus differentiated patient-derived iPSCs carrying GAT-1(S295L) into NPCs, astrocytes, and neurons and determined the GABA uptake activity. A corrected control line (corrected) was generated from the patient cell line with CRISPR/Cas9 technology and was included in every experiment as an isogenic control. Patient and corrected iPSCs as well as iPSC-derived NPCs, astrocytes and cortical inhibitory neurons were generated (Fig. 5A–D, Supplementary Fig. 3 and Supplementary Table 2) and the GABA uptake function was measured. Patient-derived cells had reduced function. A GAT-1 inhibitor Cl-966 (100 μM) was employed as control for GAT-1-mediated specific activity. Only minimal activity was detected in both iPSCs and NPCs (Fig. 5E). However, the baseline GABA activity in iPSCs was higher than the activity in untransfected HEK293T cells that was sensitive to the treatment of Cl-966 (50 μM), indicating its specificity of GABA uptake (Fig. 5F). The activity was lower in the patient cells compared with the corrected cells (70.1% ± 4.23% for patient versus 100% for corrected for iPSC; 56.15% ± 1.57% for patient versus 100% for corrected for NPC) (Fig. 5G and H). All NPCs were grown on a dense monolayer
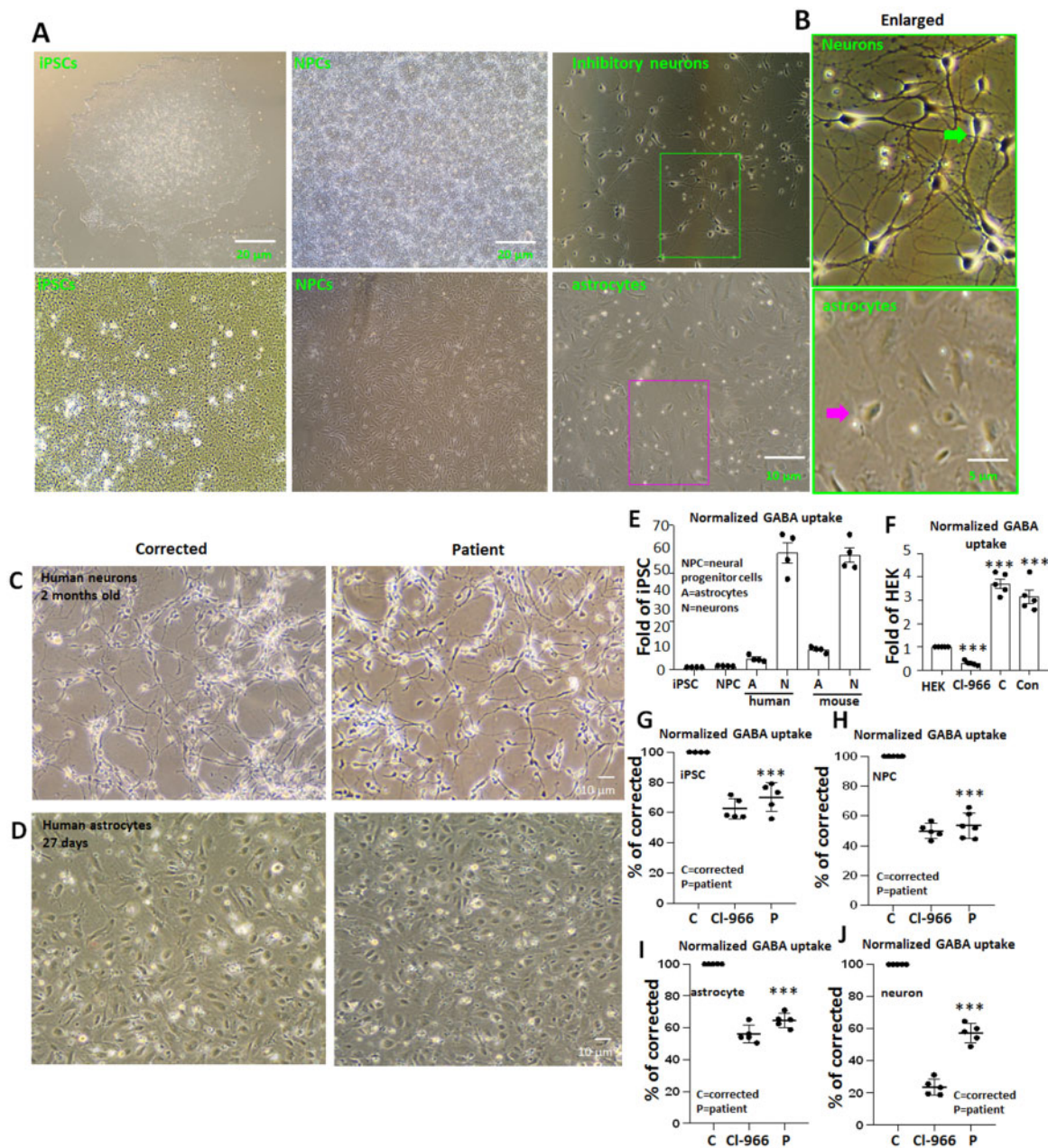
Figure 5 Altered GABA uptake function in patient iPSCs derived from astrocytes and neurons. (**A** and **B**) Representative images of live iPSCs and derived NPCs, astrocytes, and inhibitory neurons (**A**). The boxed areas in **A** are enlarged in **B**, with arrows indicating typical inhibitory neuron or astrocyte morphology. (**C** and **D**) Images of neurons or astrocytes from corrected and patient cells before GABA uptake assay. Neurons were differentiated for 60–65 days, whereas the astrocytes were differentiated for 25–30 days from NPC (P1). (**E**) The relative GABA uptake level of iPSCs, NPCs, astrocytes and neurons differentiated from human iPSCs or cultured from mouse cortices. (**F**) The relative GABA uptake level of HEK293T cells and iPSCs, where C = corrected; Con = normal control human iPSCs; Cl-966 = HEK293T cells treated with Cl-966 (50 μM) for 30 min. (**G–J**) The plots represent the reduced GABA reuptake function from patient-derived iPSCs, iPSC-derived NPCs, astrocytes and neurons measured by the high-throughput ³H radio-labelling GABA uptake on a liquid scintillator with QuantaSmart™. For iPSCs, *n* = 5 different passages. For NPCs, astrocytes and neurons, *n* = 5 experiments, with cells prepared from three different batches of cells after differentiations. NPCs were evaluated at Day 5 of P2. Astrocytes were evaluated at Day 25–30 after differentiation, and neurons were evaluated 60–65 days after differentiation. Cl-966 (100 μM) was applied 30 min before preincubation. ***$P < 0.001$ versus corrected, one-way ANOVA and Newman-Keuls test. Values are expressed as mean ± SEM.

(Supplementary Fig. 3B and C). The GABA uptake activity in differentiated astrocytes and neurons was higher than in iPSCs and NPCs, while the GABA activity in differentiated neurons was higher than in differentiated astrocytes (Fig. 5C). Compared with corrected astrocytes and neurons, the patient cells had reduced GABA uptake in both astrocytes and neurons (64.66% ± 2.04% versus 100% for corrected for astrocytes; 57.18% ± 2.64% for patient versus 100% for corrected for neurons). We increased the

concentration of Cl-966 to 100 μM because Cl-966 at a lower concentration (50 μM) only inhibited the GABA uptake activity to ∼50% in iPSCs and iPSC-derived cells. We also treated the cells with another GAT-1 inhibitor NNC-711, and a similar trend was observed, although the reduction of GABA uptake was to a lesser extent. Compared to the corrected cells, the patient cells had reduced GABA uptake activity of ∼50 to ∼70% of corrected cells across cell types (Fig. 5I to J). Considering the patient is heterozygous, the
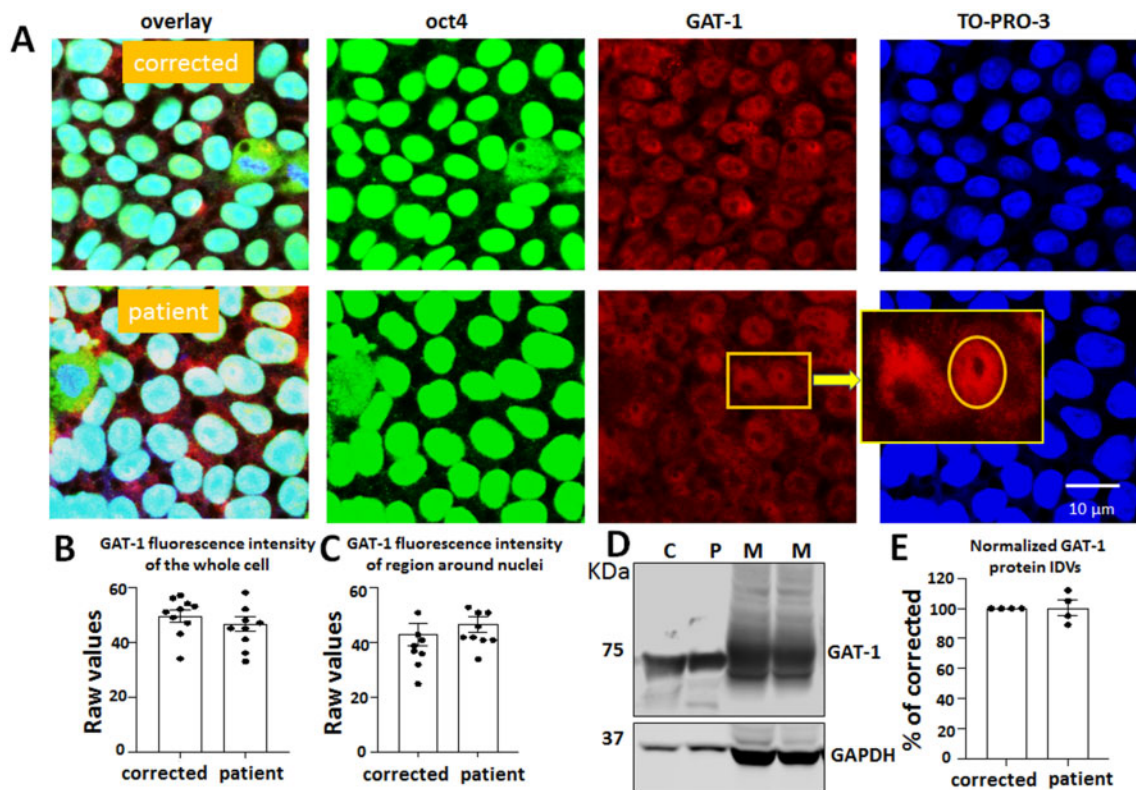
Figure 6 GAT-1 was expressed in patient-derived iPSCs. (A) The iPSCs, including the patient line [from a patient carrying the *SLC6A1(S295L)* variation] and the CRISPR corrected line (Corrected), were directly grown on Matrigel® coated glass-bottomed dishes for 2 days before staining with Oct4 (a marker for iPSCs) (mouse, 1:200) and GAT-1 (rabbit, 1:100) overnight at 4°C. Mouse IgG was visualized with Alexa-488 and rabbit IgG with Cy3. Cell nuclei were stained with TO-PRO-3 at 1:500 for 30 min. Representative images were obtained with confocal microscopy under objective 63× with zoom <2.5. The enlarged image in the *insert* shows the subcellular localization of GAT-1. **(B)** The fluorescence intensity of GAT-1 in the whole cell **(B)** or around the cell nuclei **(C)** was measured. **(D and E)** The total lysates of iPSCs or 3-month-old mouse brains were analysed by SDS-PAGE. The membrane was immunoblotted with GAT-1. C = corrected; M = mouse; P = patient. Graph represents normalized protein integrated density values (IDVs). In **E**, *n* = 4 blots. Values are expressed as mean ± SEM.

detected activity can be attributed to the wild-type allele in the patient cells.

GAT-1 has a perinuclear expression in iPSCs but has minimal GABA uptake activity

It is important to understand whether the variant GAT-1 was expressed in the iPSCs since a germline variant such as GAT-1(S295L) exists from conception on. This will provide insights into how a variant in *SLC6A1* affects cells at the stem cell stage long before they are differentiated into astrocytes or post-mitotic neurons. We co-stained the iPSCs with the iPSC pluripotency marker Oct4 and GAT-1. The cells were then stained with nuclei marker TO-PRO-3. As expected, both the patient and corrected cell lines had strong staining of Oct4, suggesting high pluripotency, though a few differentiated cells were observed (Fig. 6A). Surprisingly, GAT-1 staining also displayed a robust signal that is not, or only minimally, present in control images without the primary antibody or in HEK293T cells. A biochemical study also showed robust expression of GAT-1 in iPSCs. However, there was no difference for the total fluorescence signal of GAT-1 (49.6±2.18 for patient versus 46.6±2.8 for corrected) (Fig. 6B) and the signal around the cell nuclei region between the patient cells and the corrected lines (43±4.0 for patient versus 46.8±2.91 for corrected) (Fig. 6C). We then determined the GAT-1 expression in iPSCs with western blotting. Both the CRISPR corrected and the patient cell line had a distinct band running at ~70 kDa. Interestingly, the protein

expression pattern was different than the one observed in the adult mouse cortical tissues (Fig. 6D), suggesting different glycosylation of the GAT-1 protein in iPSCs than in adult mouse brain tissues. There was no difference in the total protein amount for the corrected and the patient iPSCs (100.3% ± 5.12% for patient versus 100% for corrected) (Fig. 6E).

The GAT-1(S295L) variant is retained intracellularly in differentiated neurons, with reduced synaptic presence

It is thought that GAT-1 is expressed in the axon terminus of GABAergic interneurons because the overall distribution pattern of neurons expressing GAT-1 is reminiscent of that of GAD- or GABA-immunoreactive neurons. Therefore, we determined the GAT-1 expression in differentiated cortical inhibitory neurons. In the rat cortex, the highest number of GAT-1 immunoreactive puncta was located in layer IV, followed by layers II–III, consistent with the distribution of interneurons. We then generated human cortical GABA inhibitory neurons. After 2 months of differentiation starting from passage 2 of NPCs, the cells displayed neuronal morphology with absence or low presence (~10%) of astrocytes in the culture. To detemine whether the differentiated neurons were mature, we co-stained the neurons with synaptic marker synaptophysin and GAT-1 (Fig. 7A–C and Supplementary Fig. 4). As expected, GAT-1 was expressed and co-localized with the synaptic marker synaptophysin.
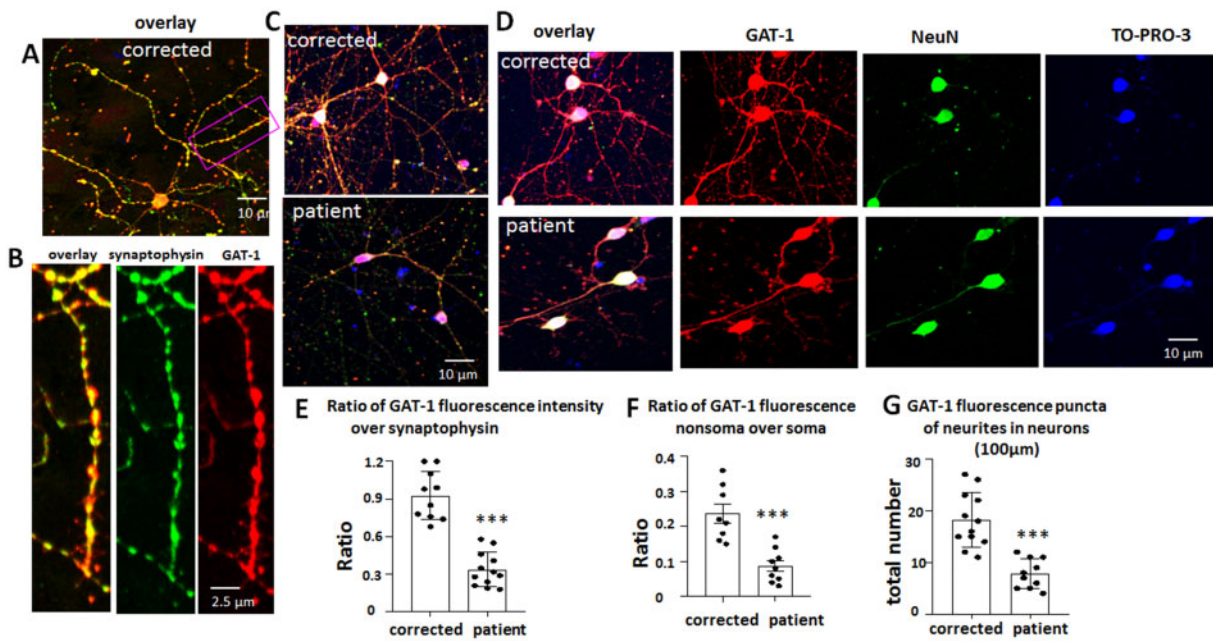
Figure 7 Variant GAT-1(S295L) was retained in neuronal soma with reduced expression in dendrites. (A–D) GABAergic inhibitory neurons (aged 60–65 days) differentiated from CRISPR corrected and patient iPSCs were immunostained with rabbit polyclonal anti-GAT-1 antibody and mouse monoclonal anti-synaptophysin (**A–C**) or anti-NeuN antibody (**D**). In **B**, the boxed region from **A** is enlarged for better synaptic visualization. The rabbit IgG was visualized with Cy3 (red) and the mouse IgG was visualized with Alexa-488 (green). The cell nuclei were stained with TO-PRO-3 (1:500). (**E**) The raw fluorescence values of GAT-1 and synaptophysin in non-somatic region were measured and the ratio was plotted. (**F**) The raw GAT-1 fluorescence values in non-somatic region and somatic regions were measured and the ratio was plotted. The soma was identified by neuronal marker NeuN. (**G**) GAT-1 fluorescence puncta in neurons differentiated from the CRISPR corrected and the patient iPSCs were quantified. The total fluorescent puncta per 100 μm was measured. In **E–G**, n = 8–12 from four batches of differentiated cells. In **E** and **F**, average raw fluorescence of GAT-1 or synaptophysin from three non-selectively chosen areas in non-somatic region was measured for each neuron. The mean value was taken as n = 1. ***P < 0.001 versus corrected, one-way ANOVA and Newman-Keuls test. Values are expressed as mean ± SEM.

We then co-stained GAT-1 with neuronal marker NeuN in differentiated neurons (Fig. 7D and Supplementary Fig. 4). The cell nuclei were stained with TO-PRO-3. Both the corrected and patient cell lines had a robust signal of GAT-1 in the neuronal soma. However, the ratio of GAT-1 fluorescent signal to synaptic marker synaptophysin was lower in the patient neurons (0.93 ± 0.06 for correct versus 0.34 ± 0.04 for patient) (Fig. 7C and E and Supplementary Fig. 4). Similarly, the ratio of GAT-1 non-somatic region to soma was lower in the patient neurons than the corrected neurons (0.23 ± 0.03 for correct versus 0.09 ± 0.015 for patient) (Fig. 7D and F). The GAT-1 puncta in the nerve endings such as dendrites or axons were lower in the patient cells than in the corrected cells (18.17 ± 1.5 for correct versus 7.8 ± 0.9 for patient) (Fig. 7D and G), suggesting a reduced presence of GAT-1 in the synapses of patient cells.

The GAT-1(S295L) variant is subject to endoplasmic reticulum-associated degradation

It has been suggested that GAT-1 is exclusively expressed in astrocytes in the thalamus of both humans and rodents.[41] Based on this suggestion, we then determined the expression of GAT-1 in differentiated human astrocytes. Human astrocytes had low baseline levels of GAT-1 expression (Fig. 8A). Compared with the corrected astrocytes, the patient astrocytes had reduced GAT-1 fluorescent signal (27.8 ± 2.44 for wild-type versus 17.3 ± 1.46 for S295L) (Fig. 8B). Interestingly, we did not identify the obvious ER retention pattern of the variant transporter in differentiated human astrocytes. The same phenomenon has been observed in GABA$_A$ receptor variants in which the ER retained variant protein becomes unnoticeable

when the variant protein is expressed with reduced abundance.[27] It is possible that the human astrocytes have the capacity to dispose of the variant protein without accumulation when the variant protein is present at a low abundance. We then transfected the human astrocytes with the wild-type and GAT-1(S295L)^{YFP} cDNAs and visualized the expression in astrocytes using live-cell imaging. Compared with the wild-type GAT-1, the variant GAT-1(S295L)^{YFP} had enhanced fluorescent signal around the nuclei, a pattern reminiscent of ER retention. The ratio of the GAT-1^{YFP} fluorescence (1.16 ± 0.11 for wild-type versus 0.30 ± 1.0.034 for S295L) in the peripheral to central region was higher in the wild-type, suggesting more GAT-1 was present at the wild-type cell surface and synapse (Fig. 8D). This suggests that the variant GAT-1 was subjected to ER-associated degradation without accumulation in the patient differentiated astrocytes. Our work also indicates the expression of GAT-1 is in low abundance in astrocytes in contrast with the expression in neurons.

Discussion

SLC6A1 pathogenic variants give rise to a wide spectrum of neurodevelopmental disorders

SLC6A1 variants are associated with a wide spectrum of neurodevelopmental disorders.[24,25,34,36] Although *SLC6A1* variants were initially described in myoclonic atonic seizures, the phenotype has been expanded to a wide spectrum including autism, childhood absence epilepsy, myoclonic astatic epilepsy, generalized tonic clonic seizures, Lennox-Gastaut syndrome, mild learning disorder, intellectual disability, and others. These clinical phenotypes
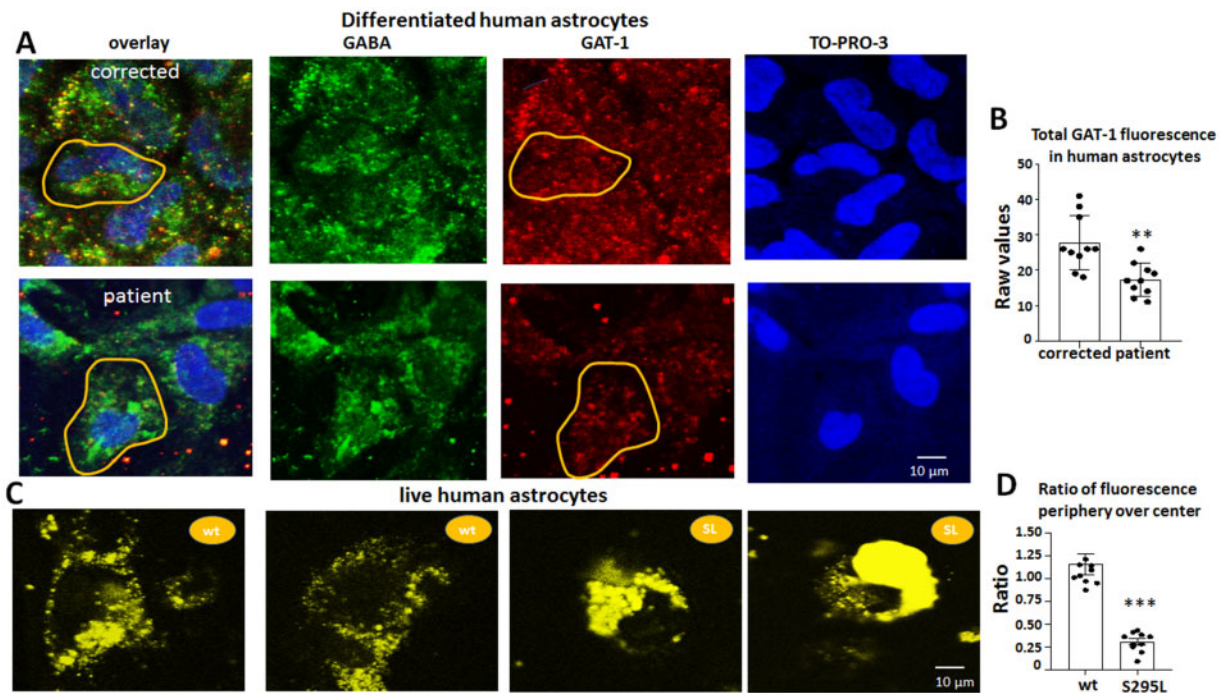
Figure 8 GAT-1 protein expression was reduced in human astrocytes at low abundance but retained inside the endoplasmic reticulum at a higher abundance. (**A**). Human astrocytes (27–30 days old) differentiated from CRISPR corrected and patient iPSCs were immunostained with rabbit polyclonal anti-GAT-1 antibody and mouse monoclonal anti-GABA antibody. The rabbit IgG was visualized with Cy3 (red), while the mouse IgG was visualized with Alexa-488 (green). The cell nuclei were stained with TO-PRO-3. The yellow circled area was arbitrarily taken as one cell and the fluorescence in the circled area was measured. (**B**) The average raw fluorescence values of GAT-1 per cell as illustrated in yellow circled area in **A** were measured. (**C**) Live human astrocytes (27–30 days old) expressing the wild-type GAT-1^{YFP} or the GAT-1(S295L)^{YFP} were visualized under confocal microscopy under objective 63×. (**D**) The GAT-1^{YFP} fluorescence in astrocytes was measured at periphery and central region as illustrated in Fig. 3A. The ratio of GAT-1^{YFP} fluorescence at the periphery versus centre was measured. In **B** and **D**, **$P < 0.01$, ***$P < 0.001$ versus wild-type, unpaired t-test. $n = 10$ from four batches of differentiated cells. Values are expressed as mean ± SEM.

overlap with those associated with GABA$_A$ receptor variants, especially those in *GABRB3* subunits.[42] This is not surprising since GABA signalling is neurotrophic during development and this signalling occurs via activation of GABA$_A$ receptors; the β3 subunit of GABA$_A$ receptors (encoded by *GABRB3*) is abundant in embryonic and young brain.[43] At a functional level, the β3 subunit is essential for pentameric receptor assembly.[44] Because GABA, GABA$_A$ receptors, and transporters work in concert to reach a dynamic homeostasis of GABA signalling that influences brain development and regulates GABAergic synaptic neurotransmission and plasticity, the defects in different components in the same pathways eventually converge and give rise to similar disease phenotypes.

Partial or complete loss of GABA reuptake is a common mechanism for *SLC6A1* variants across disease phenotypes

GAT-1 takes up GABA at the synaptic cleft; this clearance is essential in maintaining excitation/inhibition balance in the CNS. We have characterized 22 variants from patients associated with a wide spectrum of neurodevelopmental disorder phenotypes for GABA reuptake. As demonstrated in Fig. 1, it is common that variants result in reduced or complete loss of GABA uptake in HEK293T cells. The findings from cultured mouse cortical neurons and astrocytes support the data from HEK293T cells. This is also consistent with our previous study on the *SLC6A1*(G234S) variant associated with Lennox-Gastaut syndrome[24] and that on the *SLC6A1*(P361T) variant associated with epilepsy and autism.[25] The level of reduction of GABA uptake is variable, but it is consistently reduced to a level less than ∼50%. The data from human patient

iPSC-derived astrocytes and neurons also showed a reduction compared with the CRISPR-corrected isogenic control. Together, this suggests that partial or complete loss-of-function is a common mechanism for *SLC6A1* variants associated with variable phenotypes.

Loss of GABA uptake function with or without dominant negative suppression for *SLC6A1* variants

It is likely that there exist at least two pathomechanisms of loss-of-function for *SLC6A1* variants. Some variants such as *SLC6A1*(W193X) likely result in simple haploinsufficiency due to the loss-of-function of one allele while others such as *SLC6A1*(R44Q) likely result in loss-of-function plus some dominant negative suppression from the presence of the variant protein. Some variants produced minimal variant protein while others produced significant amounts of variant proteins. Additionally, some variant proteins, such as GAT-1(A288V), had reduced function, while others like GAT-1(S295L) result in almost complete loss-of-function (Supplementary Table 1). Among the surveyed variants, the cell surface expression was consistently reduced regardless of the total protein expression, suggesting that reduced functional transporter numbers at the cell surface is a common mechanism. In *GABRG2* truncation variants, we have identified that the amount of steady-state non-functional variant protein may modify the disease phenotype.[31,38,45] However, the correlation of the steady state amount of variant protein and phenotype severity for *SLC6A1* variants merits additional studies and needs to be validated in animal models.

Endoplasmic reticulum retention and associated degradation of variant GAT-1 is conserved across cell types

Misfolded variant protein is often subject to ER retention and associated degradation.[27] We have unequivocally demonstrated this in the variant GABA_A receptor subunits and some GAT-1 variants.[25,31,40] Since GAT-1 is expressed in both astrocytes and neurons, we studied the expression pattern of GAT-1 in both cell types. We found that astrocytes could serve as a viable tool for studying GAT-1 subcellular localization because of their large size and spreading cellular structure (Fig. 3). The intracellular retention of the variant protein is conserved across cell types, from HEK293T cells to astrocytes to neurons. However, while GAT-1 is expressed in iPSCs, it was not possible to identify the feature of ER retention because of the compact and aggregated morphology of iPSCs. In the differentiated GABAergic neurons, the patient cells had reduced GAT-1 puncta compared with the CRISPR corrected cells. This result is similar to our study on GABRB3 subunits with reduced synaptic distribution.[42]

The major molecular pathophysiology of variant GAT-1 is similar to dopamine and serotonin transporter variants

We hypothesize that the pathophysiology mechanisms of variants in *SLC6A1*-encoded GAT-1 are similar to those of other solute carrier family members, *SLC6A3*-encoded dopamine transporter (DAT) and *SLC6A4*-encoded serotonin transporter (SERT), both of which are better understood.[46,47] Variants in *SLC6A3* impair DAT folding, causing retention of variant DATs in the ER and subsequent reduction of transport activity. We propose that variant GAT-1 associated with various epilepsy syndromes, autism and intellectual disability cause reduced GABA transporter activity due to similar molecular defects including misfolding, ER retention and reduced transporter surface expression. Similar molecular defects are also observed for multiple variants in GABA_A receptors across subunits.[27,38] Thus, this suggests conserved molecular defects for SLC family members as well as for variants in ion channels affecting GABA pathways regardless of whether the channel is a receptor or transporter. Reduced functional transporters at the cell surface consequently lead to reduced GABA uptake activity and increased ambient GABA levels in the brain. Enhanced ambient GABA could increase tonic inhibition and give rise to absence epilepsy.[48]

Reduced GABA uptake due to loss of GAT-1 function likely contributes to absence seizures in SLC6A1 variants

We identified that GAT-1 function was reduced in both astrocytes and neurons. Absence and myoclonic atonic seizures are major seizure types observed in *SLC6A1* variants. Substantial work has been done to establish the cortico-thalamo-cortical circuitry and enhanced tonic inhibition for absence seizures. In both children and animal models of absence seizures, the ictal increase in thalamic inhibition is enhanced by the loss-of-function of GAT-1 in astrocytes. Suppressed or defective GAT-1 activity would result in increased extracellular GABA levels and thus enhanced tonic inhibition in multiple animal models for absence epilepsy.[49] Indeed, absence epilepsy has been frequently observed in patients with *SLC6A1* variants. Interestingly, previous studies indicate that the GAT-1 heterozygous knockout mouse appear phenotypically normal despite having diminished GABA reuptake activity.[12,13] Our data indicate that at least some *SLC6A1* variants, such as

SLC6A1(W193X), cause a complete loss-of-function of the variant allele and produce none to minimal variant protein. The pathophysiology of patients carrying those variants should be very similar to a heterozygous *SLC6A1* knockout. However, the patients carrying the variants manifest seizures but there are no spontaneous seizures in the heterozygous *SLC6A1* knockout mouse. This suggests that other modifying factors like the production of the variant protein[38] or genetic background[50] may contribute to clinical phenotype manifestation. Our work on *GABRG2* loss-of-function variants has provided critical insights that a small change at the molecular level may greatly modify behavioural phenotypes *in vivo*.[33,40,51]

This study has identified that the loss-of-function in *SLC6A1* is the major mechanism for epilepsy and neurodevelopmental delay associated with *SLC6A1* variants. A small cohort of *SLC6A1* variants has been associated with schizophrenia[52] but the molecular underpinning is unknown. Additionally, it is critical to understand the impact of the *SLC6A1* variants on efflux, as GABA transport is bidirectional,[53] and the impact in the context of brain development and *in vivo* during a chronic phase of phenotype evolution. It is also imperative to understand the impact of defective GAT-1 on other key components in the GABA pathway. For example, how does the impaired GAT-1 affect GAT-3 and GABA_A receptor activation? Will chronic overexposure of GABA_A receptors to GABA result in desensitization, decreasing GABA_A receptor activation? How does the variant GAT-1 affect GABA replenishment in neuronal terminals? The answers will involve using variant knock-in mice, which could provide critical insights into anti-seizure treatment and the side effects inherent to GAT-1 inhibitors, such as tiagabine. Nevertheless, this study is a step forward by proposing common mechanisms including ER retention and associated degradation, reduced surface expression, and reduced GABA uptake across variants associated with variable phenotypes and across cell types. The study provides a central piece to a large puzzle of molecular mechanisms underpinning a wide spectrum of clinical presentations for *SLC6A1* variants.

Competing interests

The authors report no competing interests.

Supplementary material

Supplementary material is available at *Brain* online.

References

1. Ben-Ari Y. Excitatory actions of gaba during development: the nature of the nurture. *Nat Rev Neurosci*. 2002;3(9):728–739.

2. Andang M, Hjerling-Leffler J, Moliner A, et al. Histone H2AX-dependent GABA(A) receptor regulation of stem cell proliferation. *Nature*. 2008;451(7177):460–464.

3. Ge S, Pradhan DA, Ming GL, Song H. GABA sets the tempo for activity-dependent adult neurogenesis. *Trends Neurosci*. 2007; 30(1):1–8.

4. Loo DD, Eskandari S, Boorer KJ, Sarkar HK, Wright EM. Role of Cl- in electrogenic Na+-coupled cotransporters GAT1 and SGLT1. *J Biol Chem*. 2000;275(48):37414–37422.

5. Sacher A, Nelson N, Ogi JT, Wright EM, Loo DD, Eskandari S. Presteady-state and steady-state kinetics and turnover rate of the mouse gamma-aminobutyric acid transporter (mGAT3). *J Membr Biol*. 2002;190(1):57–73.

6. Kang JQ. Defects at the crossroads of GABAergic signalling in generalized genetic epilepsies. *Epilepsy Res*. 2017;137:9–18.

7. Cellot G, Cherubini E. GABAergic signalling as therapeutic target for autism spectrum disorders. *Front Pediatr*. 2014;2:70-

8. Minelli A, Brecha NC, Karschin C, DeBiasi S, Conti F. GAT-1, a high-affinity GABA plasma membrane transporter, is localized to neurons and astroglia in the cerebral cortex. *J Neurosci*. 1995; 15(11):7734–7746.

9. Conti F, Melone M, De BS, Minelli A, Brecha NC, Ducati A. Neuronal and glial localization of GAT-1, a high-affinity gamma-aminobutyric acid plasma membrane transporter, in human cerebral cortex: with a note on its distribution in monkey cortex. *J Comp Neurol*. 1998;396(1):51–63.

10. Zhu XM, Ong WY. Changes in GABA transporters in the rat hippocampus after kainate-induced neuronal injury: decrease in GAT-1 and GAT-3 but upregulation of betaine/GABA transporter BGT-1. *J Neurosci Res*. 2004;77(3):402–409.

11. Jursky F, Nelson N. Developmental expression of GABA transporters GAT1 and GAT4 suggests involvement in brain maturation. *J Neurochem*. 1996;67(2):857–867.

12. Jensen K, Chiu CS, Sokolova I, Lester HA, Mody I. GABA transporter-1 (GAT1)-deficient mice: differential tonic activation of GABAA versus GABAB receptors in the hippocampus. *J Neurophysiol*. 2003;90(4):2690–2701.

13. Chiu CS, Brickley S, Jensen K, et al. GABA transporter deficiency causes tremor, ataxia, nervousness, and increased GABA-induced tonic conductance in cerebellum. *J Neurosci*. 2005; 25(12):3234–3245.

14. Carvill GL, Weckhuysen S, McMahon JM, et al. GABRA1 and STXBP1: Novel genetic causes of Dravet syndrome. *Neurology*. 2014;82(14):1245–1253.

15. Chen WJ, Lin Y, Xiong ZQ, et al. Exome sequencing identifies truncating mutations in PRRT2 that cause paroxysmal kinesigenic dyskinesia. *Nat Genet*. 2011;43(12):1252–1255.

16. Schubert J, Siekierska A, Langlois M, et al.; EuroEPINOMICS RES Consortium. Mutations in STX1B, encoding a presynaptic protein, cause fever-associated epilepsy syndromes. *Nat Genet*. 2014;46(12):1327–1332.

17. Steel D, Symonds JD, Zuberi SM, Brunklaus A. Dravet syndrome and its mimics: Beyond SCN1A. *Epilepsia*. 2017;58(11):1807–1816.

18. Stamberger H, Nikanorova M, Willemsen MH, et al. STXBP1 encephalopathy: A neurodevelopmental disorder including epilepsy. *Neurology*. 2016;86(10):954–962.

19. Picard F, Makrythanasis P, Navarro V, et al. DEPDC5 mutations in families presenting as autosomal dominant nocturnal frontal lobe epilepsy. *Neurology*. 2014;82(23):2101–2106.

20. Korenke G-C, Eggert M, Thiele H, Nürnberg P, Sander T, Steinlein OK. Nocturnal frontal lobe epilepsy caused by a mutation in the GATOR1 complex gene NPRL3. *Epilepsia*. 2016;57(3): e60–e63.

21. Gong N, Li Y, Cai G-Q, et al. GABA transporter-1 activity modulates hippocampal theta oscillation and theta burst stimulation-induced long-term potentiation. *J Neurosci*. 2009; 29(50):15836–15845.

22. Bresnahan R, Martin-McGill KJ, Hutton JL, Marson AG. Tiagabine add-on therapy for drug-resistant focal epilepsy. *Cochrane Database Syst Rev*. 2019;10(10):CD001908.

23. Scholze P, Freissmuth M, Sitte HH. Mutations within an intramembrane leucine heptad repeat disrupt oligomer formation of the rat GABA transporter 1. *J Biol Chem*. 2002;277(46): 43682–43690.

24. Cai K, Wang J, Eissman J, et al. A missense mutation in SLC6A1 associated with Lennox-Gastaut syndrome impairs GABA transporter 1 protein trafficking and function. *Exp Neurol*. 2019; 320:112973.

25. Wang J, Poliquin S, Mermer F, et al. Endoplasmic reticulum retention and degradation of a mutation in SLC6A1 associated with epilepsy and autism. *Mol Brain*. 2020;13(1):76.

26. Kang JQ, Shen W, Lee M, Gallagher MJ, Macdonald RL. Slow degradation and aggregation in vitro of mutant GABAA receptor gamma2(Q351X) subunits associated with epilepsy. *J Neurosci*. 2010;30(41):13895–13905.

27. Kang JQ, Shen W, Macdonald RL. Two molecular pathways (NMD and ERAD) contribute to a genetic epilepsy associated with the GABA(A) receptor GABRA1 PTC mutation, 975delC, S326fs328X. *J Neurosci*. 2009;29(9):2833–2844.

28. Romero-Morales AI, Robertson GL, Rastogi A, et al. Human iPSC-derived cerebral organoids model features of Leigh Syndrome and reveal abnormal corticogenesis. *bioRxiv*. [Preprint] doi:10.1101/2020.04.21.054361

29. Maroof AM, Keros S, Tyson JA, et al. Directed differentiation and functional maturation of cortical interneurons from human embryonic stem cells. *Cell Stem Cell*. 2013;12(5):559–572.

30. Keynan S, Suh YJ, Kanner BI, Rudnick G. Expression of a cloned gamma-aminobutyric acid transporter in mammalian cells. *Biochemistry*. 1992;31(7):1974–1979.

31. Kang JQ, Shen W, Zhou C, Xu D, Macdonald RL. The human epilepsy mutation GABRG2(Q390X) causes chronic subunit accumulation and neurodegeneration. *Nat Neurosci*. 2015;18(7): 988–996.

32. Kang J-Q, Kang J, Macdonald RL. The GABAA receptor gamma2 subunit R43Q mutation linked to childhood absence epilepsy and febrile seizures causes retention of alpha1beta2gamma2S receptors in the endoplasmic reticulum. *J Neurosci*. 2004;24(40): 8672–8677.

33. Warner TA, Shen W, Huang X, Liu Z, Macdonald RL, Kang JQ. DIfferential molecular and behavioral alterations in mouse models of GABRG2 haploinsufficiency versus dominant negative mutations associated with human epilepsy. *Hum Mol Genet*. 2016;25(15):3192–3207.

34. Carvill GL, McMahon JM, Schneider A, et al.; EuroEPINOMICS Rare Epilepsy Syndrome Myoclonic-Astatic Epilepsy & Dravet working group. Mutations in the GABA transporter SLC6A1 cause epilepsy with myoclonic-atonic seizures. *Am J Hum Genet*. 2015;96(5):808–815.

35. Johannesen KM, Gardella E, Linnankivi T, et al. Defining the phenotypic spectrum of SLC6A1 mutations. *Epilepsia*. 2018;59(2): 389–402.

36. Mattison KA, Butler KM, Inglis GAS, et al. SLC6A1 variants identified in epilepsy patients reduce gamma-aminobutyric acid transport. *Epilepsia*. 2018;59(9):e135–e141.

37. Richards S, Aziz N, Bale S, et al.; ACMG Laboratory Quality Assurance Committee. Standards and guidelines for the interpretation of sequence variants: Joint consensus recommendation of the American College of Medical Genetics and Genomics and the Association for Molecular Pathology. *Genet Med*. 2015; 17(5):405–424.

38. Kang JQ, Shen W, Macdonald RL. Trafficking-deficient mutant GABRG2 subunit amount may modify epilepsy phenotype. *Ann Neurol*. 2013;74(4):547–559.

39. Zhang CQ, McMahon B, Dong H, et al. Molecular basis for and chemogenetic modulation of comorbidities in GABRG2-deficient epilepsies. *Epilepsia*. 2019;60(6):1137–1149.

40. Kang JQ, Macdonald RL. Molecular pathogenic basis for GABRG2 mutations associated with a spectrum of epilepsy syndromes, from generalized absence epilepsy to Dravet syndrome. *JAMA Neurol*. 2016;73(8):1009–1016.

41. De BS, Vitellaro-Zuccarello L, Brecha NC. Immunoreactivity for the GABA transporter-1 and GABA transporter-3 is restricted to astrocytes in the rat thalamus. A light and electron-microscopic immunolocalization. *Neuroscience*. 1998;83(3):815–828.

42. Shi YW, Zhang Q, Cai K, et al. Synaptic clustering differences due to different GABRB3 mutations cause variable epilepsy syndromes. *Brain*. 2019;142(10):3028–3044.

43. Tanaka M, DeLorey TM, Delgado-Escueta A, Olsen RW. *GABRB3*, Epilepsy, and Neurodevelopment. In: Noebels JL, Avoli M, Rogawski MA, Olsen RW, Delgado-Escueta AV, eds. *Jasper's Basic Mechanisms of the Epilepsies*. 4th ed. Bethesda (MD): National Center for Biotechnology Information (US); 2012.

44. Connolly CN, Krishek BJ, McDonald BJ, Smart TG, Moss SJ. Assembly and cell surface expression of heteromeric and homomeric gamma-aminobutyric acid type A receptors. *J Biol Chem*. 1996;271(1):89–96.

45. Wang J, Shen D, Xia G, et al. Differential protein structural disturbances and suppression of assembly partners produced by nonsense GABRG2 epilepsy mutations: Implications for disease phenotypic heterogeneity. *Sci Rep*. 2016;6:35294.

46. Asjad HMM, Kasture A, El-Kasaby A, et al. Pharmacochaperoning in a Drosophila model system rescues human dopamine transporter variants associated with infantile/juvenile parkinsonism. *J Biol Chem*. 2017;292(47):19250–19265.

47. Mergy MA, Gowrishankar R, Gresch PJ, et al. The rare DAT coding variant Val559 perturbs DA neuron function, changes behavior, and alters in vivo responses to psychostimulants. *Proc Natl Acad Sci U S A*. 2014;111(44):E4779–E4788.

48. Cope DW, Di GG, Fyson SJ, et al. Enhanced tonic GABAA inhibition in typical absence epilepsy. *Nat Med*. 2009;15(12):1392–1398.

49. Crunelli V, Leresche N, Cope DW. GABA-A Receptor Function in Typical Absence Seizures. In: Noebels JL, Avoli M, Rogawski MA, Olsen RW, Delgado-Escueta AV, eds. *Jasper's Basic Mechanisms of the Epilepsies*. 4th ed. Bethesda (MD): National Center for Biotechnology Information (US); 2012.

50. Mistry AM, Thompson CH, Miller AR, Vanoye CG, George AL Jr, Kearney JA. Strain- and age-dependent hippocampal neuron sodium currents correlate with epilepsy severity in Dravet syndrome mice. *Neurobiol Dis*. 2014;65:1–11.

51. Xia G, Pourali P, Warner TA, Zhang CQ, Macdonald L, Kang JQ. Altered GABAA receptor expression in brainstem nuclei and SUDEP in Gabrg2(+/Q390X) mice associated with epileptic encephalopathy. *Epilepsy Res*. 2016;123:50–54.

52. Rees E, Han J, Morgan J, et al. GROUP Investigators. De novo mutations identified by exome sequencing implicate rare missense variants in SLC6A1 in schizophrenia. *Nat Neurosci*. 2020;23(2):179–184.

53. Sitte HH, Singer EA, Scholze P. Bi-directional transport of GABA in human embryonic kidney (HEK-293) cells stably expressing the rat GABA transporter GAT-1. *Br J Pharmacol*. 2002;135(1):93–102.